LoRa performance in industrial environments: analysis of different ADR algorithms

Angelo Soto-Vergel, Luis Arismendy, Robinson Bornacelli-Durán, Carlos Cardenas, Brayan Montero-Arévalo, Emanuel Rivera, Maria Calle, *Senior Member, IEEE*, John E. Candelo-Becerra, *Member, IEEE*

***Abstract*— LoRaWAN (Long Range Wide Area Network) technology can be a good candidate for industrial applications in IoT and Adaptive Data Rate (ADR) algorithms help to improve LoRaWAN performance. These algorithms compute a link budget to define the data rate and the transmission power. However, the performance of these algorithms must be evaluated in industrial environments that pose challenging conditions to wireless communications due to obstacles, interference, and movement. Therefore, this article compares the performance of LoRaWAN with six different ADR algorithms using a realistic propagation model from an industrial environment. The research uses the FLoRa environment in Omnet++ to compare the packet delivery ratio and energy consumption with different gateway locations and data traffic. Results show that the algorithms that decrease the link budget in poor channel conditions have better performance in industrial scenarios. Furthermore, overestimating the channel behavior decreases packet delivery.**

***Index Terms*—Adaptive data rate, packet delivery ratio, energy consumption, propagation model, industrial applications**

I. Introduction

THE Internet of Things (IoT) shows potential for exploiting Industry 4.0 in the construction of smart cities and in industrial growth. IoT impacts everything from machine-to-machine communication to data collection for implementing smart solutions [1]. However, industrial environments have obstacles and interference from different sources that affect communication between nodes [2]. Additionally, Industrial IoT requires wireless networks with low power consumption, low cost, robustness to interference, long radio range, and coverage with large node densities [3].

LoRaWAN, developed by LoRa Alliance, is one technology matching all these features [4], especially by using the Adaptive Data Rate (ADR). This characteristic modifies the node data rate according to channel conditions to improve energy consumption and packet delivery [5]. Various authors have studied and improved the performance of the original ADR for different network conditions with static or mobile nodes [6]. Most studies strived to mitigate effects on the network, such as packet loss [5], collisions [7], and others due to channel variability [8]. These studies employed radio propagation models obtained from different scenarios, usually outdoors urban [5], [6], [7], or sub-urban [5].

Even though the literature presents different propagation models, it is not clear if they match industrial environments. These facilities are usually indoors and exhibit characteristics that affect signal propagation. Some examples are building layout, the presence of machines and highly reflective surfaces, such as metallic structures [9]. Moreover, few studies such as [10] work on testing the performance of LoRaWAN in industrial conditions. Furthermore, the papers do not mention specific applications that could employ these ADR algorithms.

Hence, this paper aims to test diverse ADR algorithms with realistic industrial propagation conditions, showing applications that may benefit from these algorithms.

Thus, the main contributions of this paper are:

- The paper creates a novel propagation model for a worst-case scenario for LoRa communications in industrial settings based on measurements from [10].
- The paper determines the characteristics that improve ADR energy usage and packet delivery for industrial environments.
- According to this performance, the paper provides recommendations for using the algorithms in diverse industrial applications.

The paper is organized as follows. Section II introduces the main characteristics of LoRa and the ADR mechanism. Section III describes related work focused on two topics: different algorithms for improving ADR and propagation models for industrial environments. Section IV details the tests and conditions for the evaluation of the selected algorithms. The following section presents the tests and analyzes the results. Finally, section VI concludes the paper.

This paragraph of the first footnote will contain the date on which you submitted your paper for review, which is populated by IEEE.

Corresponding author: Maria Calle

Angelo Soto-Vergel is with the Universidad Francisco de Paula Santander, Cúcuta, 540003, Colombia and the Universidad del Norte in Barranquilla, 080001, Colombia (jvergela@uninorte.edu.co).

Luis Arismendy, Robinson Bornacelli-Durán, Carlos Cardenas, Emanuel Rivera and Maria Calle are with the Universidad del Norte, Barranquilla, 080001, Colombia. (e-mails: arismendyl, rbornacelli, ccarlosa, remanuel, mcalle @uninorte.edu.co).

Brayan Montero-Arévalo is with the Universidad Nacional de Colombia in La Paz, 202010, Colombia (brayanmontero@uninorte.edu.co).

John E. Candelo-Becerra is with the Universidad Nacional de Colombia, Sede Medellín. Medellín, 050041, Colombia (jecandelob@unal.edu.co).

II. Background

A. LoRa

LoRaWAN is a wireless technology to provide long-range communication with robustness against noise [11]. Both Medium Access Control (MAC) and the network layer of LoRaWAN work over LoRa, the physical layer specification. LoRa uses the Chirp Spread Spectrum (CSS) modulation patented by Semtech. LoRaWAN provides bidirectional communication at long distances with data rates below 27 kbps on the industrial, scientific, and medical radio bands (ISM) [12]. Five important LoRa parameters are transmission power (TP), bandwidth (BW), code rate (CR), spreading factor (SF), and center frequency. BW is the range of frequencies, CR provides error correction, and SF indicates the information spreading over time. These parameters affect radio range, time on-air (ToA), noise robustness, data rate (DR), and decoding at the receiver [13].

The data rate (R_b) is given by (1) [14]. The term SF is an integer value between 7 and 12. The term BW has values of 125, 250, or 500 kHz.

$$R_b = \mathrm{SF} * \frac{1}{\frac{2^{\mathrm{SF}}}{\mathrm{BW}}} \quad (1)$$

A higher SF means a lower data rate, smaller sensitivity, and longer radio range. For illustration, Table I shows sensitivity and the required SNR for SF 7 and 12 with BW of 125kHz [15].

TABLE I.
SENSITIVITY VALUES FOR SF7 AND SF12, 125 KHZ [15]

SF	Sensitivity [dBm]	Required SNR [dB]
7	-124.5	-7.5
12	-137.0	-20

SF also impacts the frame duration when transmitted (ToA) because this metric depends upon symbol duration as shown in (2) [16].

$$\mathrm{ToA} = T_{sym} * [(n_{preamble} + 4.25) + payloadSymbNb] \quad (2)$$

The term $n_{preamble}$ is the number of symbols in the preamble, $payloadSymbNb$ is the number of symbols in the payload, and T_{sym} is the symbol duration, given in (3). Therefore, the frames spend more time on air when the device uses a larger SF.

$$T_{sym} = \frac{2^{\mathrm{SF}}}{\mathrm{BW}} \quad (3)$$

LoRaWAN nodes can transmit through several kilometers. However, the technology exhibits packet losses in the presence of obstacles, even for distances of hundreds of meters [3]. The technology uses a star-of-stars topology; thus, the nodes send information to one or more gateways within their coverage area. Then, the gateways send the information to a network server (NS) using Internet connections [2].

Additionally, LoRaWAN works with three types of devices:

- Class A nodes employ mainly uplink (from node to gateway) communication and devices only listen for downlink traffic after uplink transmissions [2].
- Class B devices listen for downlink packets at different time slots. Thus, nodes exhibit larger energy usage than class A devices [2].
- Class C devices will listen continuously for downlink traffic unless they open uplink windows. Consequently, they will consume more energy than Class A and B [2].

B. ADR functionality

The Things Network (TTN) adopted a mechanism considered the standard ADR (ADR-TTN) that defines LoRaWAN transmission parameters dynamically. Semtech Corporation proposed ADR-TTN with two different algorithms, one in the node and the other in the server. The node algorithm increases SF (and radio range) when there are no downlink transmissions after several uplink messages. The server algorithm counts the last (commonly 20) received packets, computing the maximum Signal-to-Noise-Ratio (SNR) value. Then, the algorithm computes a Link Budget by using (4) [17].

$$\text{Link Budget} = SNR_e - SNR_r - margin\_db \quad (4)$$

Where SNR_e is the SNR value computed from the last N packets, SNR_r is the SNR required for successful demodulation, and $margin\_db$ is an error margin (typically 10 dB).

The result of this computation helps to determine SF and TP [10]. Fig. 1 illustrates the three main Server ADR concepts: SNR evaluation, link budget calculation, and transmission parameter estimation (SF and TP).

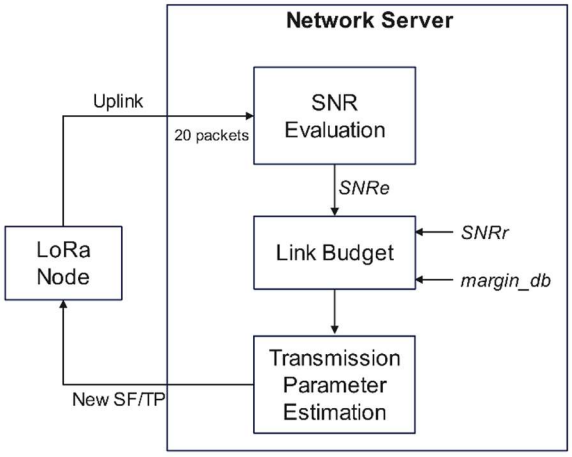

Fig. 1. General ADR algorithm.

By changing SF and TP, ADR algorithms help the network to reduce the number of lost packets and decrease energy consumption [5]. However, ADR convergence time to reach the optimum data rate may span hours or days [6]. From now on, this paper refers to ADR-TTN as ADRmax, to denote the selection of the maximum SNR value in the SNR evaluation section of the algorithm.

III. Related Work

A variety of ADR algorithms are present in the literature, each one seeking to improve a specific characteristic. This section reviews different studies for improving ADRmax and diverse propagation models for industrial scenarios.

A. ADR Algorithms

The following algorithms try to improve the packet delivery ratio (PDR) and energy consumption of ADRmax.

1) ADR+

This algorithm uses the average SNR of the last 20 packets to estimate TP and SF [5]. The paper evaluates ADR+ within the FLoRa framework in Omnet ++. Results show that ADR+ outperforms ADRmax and No ADR (not using ADR) at least 30% in energy consumption. Additionally, ADR+ obtains better PDR when the channel has higher variability.

2) ADRx

This mechanism uses the average SNR of the last 20 uplinks, as ADR+ [8]. Additionally, ADRx modifies the margin_db to improve the estimation of the channel conditions and the link quality. As a result, ADRx offers low energy consumption as ADR+, decreasing convergence times at least four times.

3) ADRmin

The algorithm uses the minimum SNR value of the last 20 packets received to estimate SF and TP [18]. The study uses simulations with Omnet ++ and compares ADRmin with ADRmax and ADR+. ADRmin improves four times the PDR and improves energy consumption in scenarios with very noisy channels.

4) ADR Gauss and EMA-ADR

Gaussian filter ADR (ADR Gauss) models the SNR values as a Gaussian probability density function (PDF) for determining TP and SF [6]. The same study proposes exponential moving average ADR (EMA-ADR). The method uses a weighted moving average of the SNR to smooth the SNR peaks, improving the estimation of TP and SF. As a result, both mechanisms improve ADRmax performance in energy consumption and packet delivery with static and mobile nodes.

5) Other ADRs

The literature presents other options to improve ADR performance regarding PDR considering collisions [7], energy efficiency related to the data rate [19], [16], and convergence time [21]. In these papers, the performance of these algorithms is usually compared to ADRmax. Additionally, the literature shows different works that do not present quantitative comparisons with this method, such as [22], [18], [24], and [25].

A different approach studies ADR in industrial scenarios using class B devices. The study uses simulations to analyze ADR in uplink and downlink transmissions [26].

6) ADR selection

The majority of the previous works improved on the original ADR algorithm employing class A devices, the most energy efficient in LoRaWAN [2]. Additionally, class A is mandatory for all LoRa devices [28]. Hence, ADR algorithms for this class can be implemented in all commercial LoRa systems. However, the reviewed papers with this class do not evaluate their approaches in industrial scenarios. Moreover, the papers do not provide specific example applications that can benefit from the algorithms.

Industrial wireless applications have different requirements such as small energy usage and large packet delivery [27]. Moreover, industrial facilities span hundreds of meters, have variable communication channels and require a multitude of nodes. Therefore, our study employs ADR algorithms designed to improve energy usage and PDR in class A devices. Additionally, our experiments must use algorithms that have been tested with conditions comparable to those expected in industrial environments. Therefore, the algorithms that comply with these criteria are ADRmax, ADR+, ADRmin, ADRx, ADR Gauss, and EMA-ADR.

B. Propagation Models for Industrial Environments

Wireless communications in industrial environments face obstacles, movement, and interference from different sources. Thus, different authors performed measurement studies to obtain propagation models of these environments. This section includes tests performed in industrial environments as follows: first with non-LoRa devices, then with simulations of LoRa devices and finally with field tests including LoRa nodes.

1) Non-LoRa tests

One example study uses a signal generator as the transmitter and a spectrum analyzer as the receiver. The tests include continuous-wave signals at 900 MHz, 2.4 GHz, and 5.2 GHz [9]. A similar study uses 2.4 and 5.2 GHz [29]. However, these studies do not use LoRa, and the physical layer can create radio propagation differences.

2) LoRa simulations

Different papers employ simulations of LoRa in industrial settings. One example uses the Hybrid path loss in buildings, available for ns-3 with Class B LoRaWAN devices [26]. The model combines different outdoors models (COST231 and Okumura–Hata), and the ITU-R P.1238 indoor model. Another example model used in industrial simulations is the LoRa log-normal with obstructions, available for FLoRa in Omnet++ [30]. The work in [5] describes this model, originally derived for outdoors, sub-urban environments.

The models in the literature use the general path loss model defined in (5) [9], [29]. with different values depending on the scenario.

$$PL(d) = PL(d_0) + 10 * \gamma * log_{10}\left(\frac{d}{d_0}\right) + X_\sigma \qquad (5)$$

Where:
$PL(d_0)$: is the path loss for a reference distance d_0.
γ: is the path loss exponent.
d: is the distance to calculate the path loss.
X_σ: is a random variable with normal distribution, zero mean, and standard deviation σ. This variable represents the shadowing/fading component.

Table II shows the worst-case obtained from the different models presented in the literature, given by the largest value of the path loss exponent. Table II shows path loss exponents from 2.32 to 3.0 in the LoRa frequency range (Refs. [9], [26], and [5]). However, it is not clear if these models accurately represent LoRa behavior in industrial environments.

TABLE II
SUMMARY OF PATH LOSS MODELS FOR INDUSTRIAL ENVIRONMENTS

Ref	Frequency (MHz)	d_0[m]	$PL(d_0)$[dB]	γ	σ [dB]
[9]	900	15	61.65	2.49	7.35
[29]	2300	1	42.6	2.8	7.6
[26]	868	NA	58.77	3.0	-13.0
[5]	868	1000	128.95	2.32	7.08

3) LoRa tests

To the best of our knowledge, there are two studies with results from LoRa tests in industrial environments. The first study measures RSSI and SNR for nodes with a range extender in an industrial laboratory [31]. However, the paper does not provide the distances; thus, there is no way to compute a propagation model. The other study measures RSS and SNR of nodes located at different distances with LOS (Line-of-Sight) and NLOS (Non-Line-of-sight) conditions [10]. The study shows the locations of the nodes with the distances to the gateway; nonetheless, the paper does not include path loss models. Results show that packet losses are 0.5% for SF7 and SF12 with all devices inside the warehouse. However, if the gateway stays inside and the nodes move outside, it is possible to receive packets only with SF7, and packet losses increase to 6%. All other SFs show 100 % packet losses even with 400 m distances, shorter than LoRa maximum range. These results confirm that obstacles and walls significantly affect LoRa transmissions, as presented in [32]. Hence, it is necessary to create and verify new propagation models for LoRa in industrial environments.

IV. EXPERIMENTS

This section describes the computation of the propagation model for industrial environments. Then, we present the performance metrics and all the variables used in the simulation. Experiments use the FLoRa framework with Omnet++ and INET 4.3.

A. Realistic propagation model for industrial environments

This work uses RSSI measurements from [10] to create a realistic path loss model for LoRa in industrial scenarios. The measurements use one node transmitting to one gateway with 14 dBm transmission power and 868 MHz. The test area is a warehouse of 190 m x 180 meters with moving carts for transporting flowers. The tests locate the node at different places in two measurement locations at the warehouse: the sideways and the ground floor. The latter includes NLOS conditions, has longer distances and smaller RSSI values than the former. Thus, we selected the ground floor as worst-case scenario to compute a path loss model for demanding industrial environments.

The paper [10] does not include the direct distances between each test location and the gateway nor the path losses. Hence, we computed the Euclidean distances between every node position and the gateway. Then, we employed the classical method used for estimating path loss models in studies such as [9] and [29]. The method includes the following steps: the first step determines the path losses by subtracting the received signal from the transmission power (14 dBm). Table III shows the results for the worst-case presented in [10].

TABLE III
LOSSES IN AN INDUSTRIAL ENVIRONMENT COMPUTED FROM [10]

Location	Euclidean Distance (m)	Path Loss [dB]		
		Min	Average	Max
L7	78.3	91	97	113
L8	96.6	95	104	122
L9	115.4	98	109	121
L10	134.6	104	108	119
L11	154.0	106	111	119
L12	173.6	104	114	133

The following step is to determine the values in (5) employing the results in Table III and the recommendations in [9]. Hence, the method computes a least-squares fit of the path losses and the logarithm of the distance. This fit provides the values of $PL\ (d_0)$ and γ from (5). The last step is calculating σ as the standard deviation of the residuals of each measurement respect to the least squares fit, as described in [29].

Finally, Table IV shows the specific model of LoRa at 868 MHz in industrial environments. The table shows double path loss and a larger shadowing component than those presented in Table II. Thus, Table IV demonstrates the difference between the worst-case scenarios from the literature and the industrial setting for LoRaWAN.

TABLE IV
PROPAGATION MODEL PARAMETERS IN THE INDUSTRIAL ENVIRONMENT

d_0[m]	$PL(d_0)$[dB]	γ	σ[dB]
1	14.7	4.4	9.6

Regarding model validation, Fig. 2 shows the minimum, average and maximum measured values (blue, orange, and gray markers). The figure also illustrates the simulated path losses using the model created in this work (green triangles). According to the figure, the model covers the minimum and average values, and even some of the maximum. Thus, it can be helpful for analyzing the behavior of LoRa systems in industrial scenarios similar to [10].

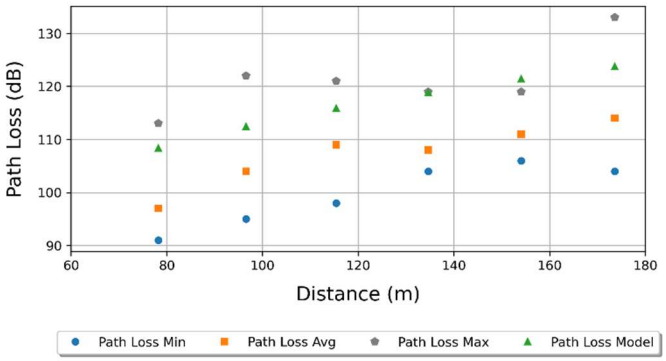

Fig. 2. Industrial Path Loss model and the measured values.

B. Simulation Setup

The industrial test environment is a rectangle of 2000 m x 500 m. The area is consistent with a large industrial setting such as an automobile manufacturing plant, as in [29]. Tests do not include walls because they create significant packet losses with most SF values, as shown in [10]. The nodes are located randomly with uniform distribution. The tests initially select a random SF value for each node and the maximum transmission power. This value is 14 dBm to guarantee communication with the server. Fig. 3 illustrates the network topology of the scenario using a server connected to a gateway via a cloud

connection.

The system uses a 125 kHz bandwidth with 4/8 code rate as in [5], to maximize protection against errors. The setup also includes two gateway locations: the center and one corner. The center case decreases the average distance to the nodes. However, locating the gateway at the center in an industrial setup may not be feasible or practical. Thus, experiments also locate the gateway in a corner to better reflect a real-life worst-case situation.

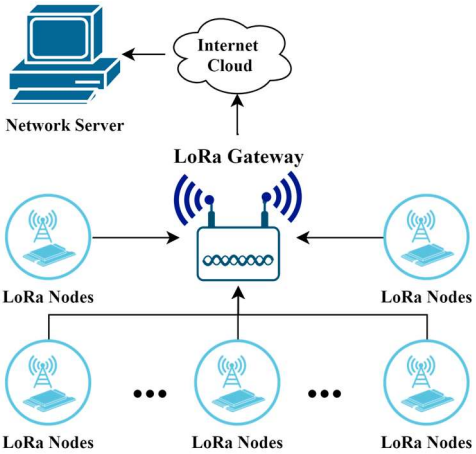

Fig. 3. Network topology.

The simulations employ networks from 100 to 1000 nodes. As an illustration, Fig. 4 shows examples of networks with 100 and 500 nodes with each gateway location.

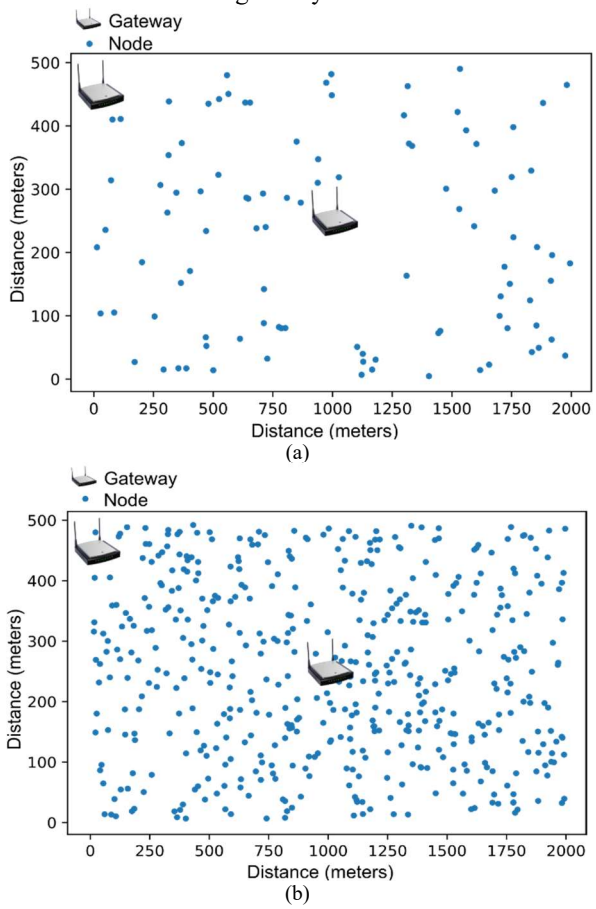

Fig. 4. Example node locations with (a) 100 and (b) 500 nodes. Every test used only one gateway located at the corner or the center of the test area.

The simulation time for each experiment is five days and includes all the energy and packets. This way, the simulation includes the network transient state to evaluate the response of all ADRs under the same conditions. Hence, the simulation reflects the actual situation in an industrial setting. Additionally, simulations include 10 different random networks with each number of nodes and algorithms.

Each node sends a packet with 51 bytes in the application payload, the maximum for DR 0 to 12 in the 868 MHz Band [33]. Other data rates allow for larger payloads; however, ADR modifies DR; thus, nodes can send 51-bytes packets in all DRs.

The simulation sends the packets at time intervals modeled by an exponential distribution. The nodes do not send retransmissions to determine the minimum PDR achievable with the smallest energy consumption. Experiments use one and ten packets per hour to evaluate the algorithms for different applications with low and high traffic. Some example applications with the former are smart metering, alarm, and event detection. Regarding the latter, industrial applications include inventory, remote equipment monitoring, and quality control.

Table V summarizes the factors and levels from the experimental design of this work. Tests use a total of six different ADR implementations and one case without ADR.

TABLE V
SIMULATION DATA

Factors	Levels
ADR Algorithm	No ADR ADRmax ADR+ ADRx ADRmin ADR Gauss EMA-ADR
Number of nodes	100 to 1000 in steps of 100
Packets per hour	1, 10
Gateway location	Center, Corner

C. Network Performance Metrics

Consistent with the algorithm selection criteria, this paper compares ADR performance using the metrics in [5] and [6]:

- *Packet delivery ratio (PDR):* the number of packets successfully received at the server (RxS) divided by the messages transmitted by all nodes (TxNodes). Thus, *PDR* is:

$$PDR = RxS / TxNodes \quad (6)$$

FLoRa tests assume that a transmission is successful if the received signal power is greater than the receiver sensitivity. The system also accounts for collisions when nodes send frames at the same time in non-orthogonal channels. Furthermore, experiments include the capture effect. Hence, the gateway receives the strongest of two simultaneous signals with two conditions. The first condition is a difference of at least 6 dB between both signals. The second condition is the gateway detecting a minimum of five symbols in the preamble [5].

- *Energy consumption per received packet:* the total energy employed by all nodes (ENodes) divided by the number of packets successfully received at the server. Thus, $Energy_{rx}$ is:

$$Energy_{rx} = ENodes / RxS \quad (7)$$

V. Results and Analysis

This section presents the simulation results according to the parameters in Table V. The section compares the performance of the algorithms regarding PDR and energy consumption per packet received. This information is helpful for designers and engineers to select the appropriate algorithm according to the application. All charts show average values with 95% confidence intervals.

A. Packet Delivery Ratio

Fig. 5 illustrates the percentage of packets delivered correctly as a function of the number of active nodes. The figure shows the results with the gateway centered on the area (a) and the corner (b). Both scenarios show that PDR is similar when the number of nodes increases between 100 and 1000. Hence, all algorithms scale well in low traffic conditions. However, PDR decreases by 20% with the gateway in the corner. This result is a consequence of the corner gateway having larger distances to the nodes.

Fig. 5 also shows that PDR for ADRmax is the lowest among the implemented algorithms in both gateway positions. The situation is due to ADRmax using the maximum SNR value for computing SF and TP. This strategy overestimates the channel behavior and establishes SF and TP as if most packets have large SNR. However, the high variability of the industrial environment decreases SNR in the packets affecting PDR.

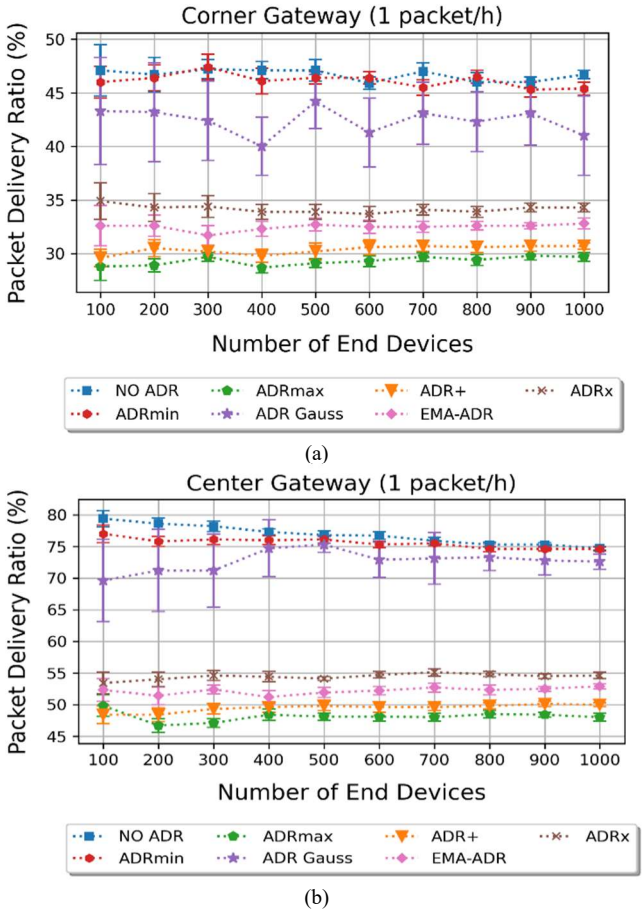

Fig. 5. PDR by number of nodes with one packet/hour. (a) corner gateway (b) center gateway.

Additionally, according to Fig. 5, No ADR, ADRmin and ADR Gauss exhibit larger PDR values than the other algorithms. The situation is due to starting the transmission with random SF values and maximum TP, helping to deliver more packets. Moreover, using the minimum SNR value (ADRmin) or a Gaussian filter (ADR Gauss) yield similar results with low traffic. The situation is due to ADRmin decreasing the link budget if the channel is poor as in industrial environments. Furthermore, a particular case occurs with ADR Gauss where the calculation of SNR uses a Gaussian PDF. The algorithm updates this PDF in each iteration and discards the data outside the distribution. Thus, the method decreases the number of values used to calculate the final average.

Regarding applications, the maximum PDR achieved in low traffic was 80%; thus, applications in similar conditions must tolerate packet losses, such as smart metering. On the other hand, applications like event and alarm detection must deliver all packets; therefore, they require methods with 100% PDR.

Fig. 6 illustrates the results with high traffic (10 packets/hour). Again, PDR for the center gateway is better than the corner gateway. However, Fig. 6 shows a decreasing trend for the four better algorithms as the number of nodes increases. The behavior is due to the increased network traffic, raising the packet collisions in LoRaWAN, thus decreasing PDR. The result is consistent with [5], showing that PDR is a function of the number of active nodes in the network and traffic. The result is due to the ALOHA-type protocol employed in LoRaWAN.

According to Fig. 6, ADRmax exhibits the lowest performance again. The result is due to channel overestimation; additionally, the other algorithms were designed to improve ADRmax performance. Furthermore, Fig. 6 shows similar results of ADR+ and EMA-ADR for both gateway locations, consistent with Fig. 5. Nonetheless, high traffic decreases PDR when compared to low traffic.

Furthermore, when comparing Figs. 5(a) and 6(a) all ADR decrease PDR with high traffic except for ADRmin and ADRx. These algorithms compute their link budget by using the minimum SNR and modifying the margin_dB value, respectively. Note that all algorithms require 20 uplinks to update the SF and TP values. Consequently, convergence time is longer when sending one packet per hour than it is with 10 packets per hour. This situation should benefit all algorithms in high traffic. However, Figs. 5(a) and 6(a) show that ADRmin and ADRx increase PDR, while the other algorithms decrease. Therefore, the link budgets in ADRmin and ADRx adapt better to this channel than all other algorithms in high traffic.

Concerning applications, the best PDR is 80% only up to 100 nodes. Therefore, the technology is adequate if the application tolerates packet losses, such as remote equipment monitoring. Additionally, No ADR exhibits significantly less PDR than other options. Thus, high traffic applications will benefit from using an ADR algorithm. Furthermore, Fig. 6 shows that ADRx obtains the best performance with the gateway in the center, very close to ADRmin. On the corner gateway, ADRmin has better performance with more than 300 nodes. Since ADRmin also has better performance in low traffic, the algorithm may be a good option regardless the type of traffic.

This article has been accepted for publication in IEEE Transactions on Industrial Informatics. This is the author's version which has not been fully edited and content may change prior to final publication. Citation information: DOI 10.1109/TII.2023.3240696

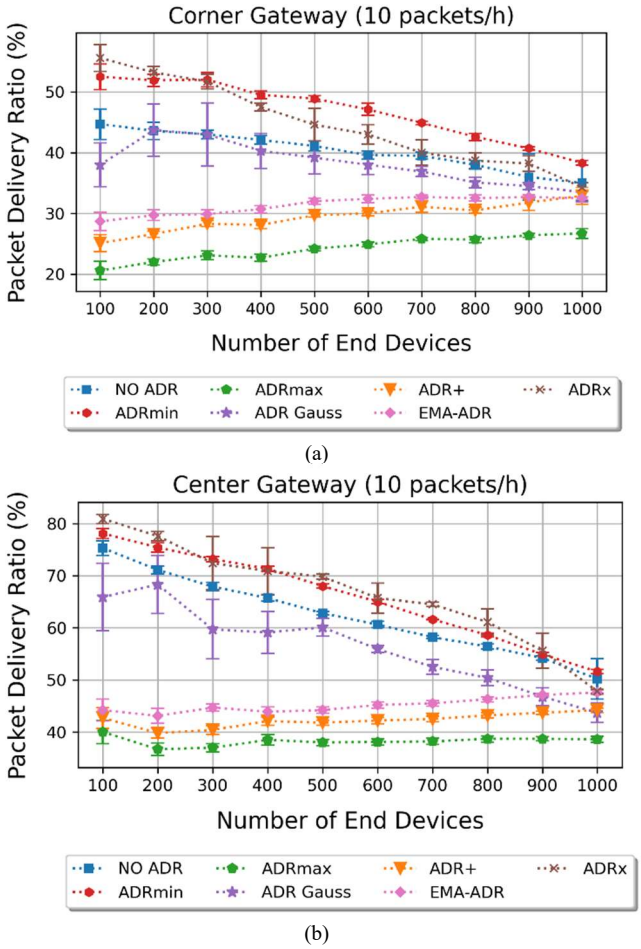

Fig. 6. PDR by number of nodes with ten packets/hour. (a) corner gateway (b) center gateway.

B. *Energy Consumption per received packet*

Fig. 7 illustrates the average consumption per received packet for the low traffic case. No ADR exhibits the largest energy consumption as expected. The situation is due to all nodes starting with the maximum TP and not changing throughout the simulation. All other methods modify the TP and SF values, helping to save energy. Additionally, ADRmin obtains the smallest energy usage in both gateway locations with a good PDR in low traffic; hence, the algorithm may represent an interesting balance between both metrics.

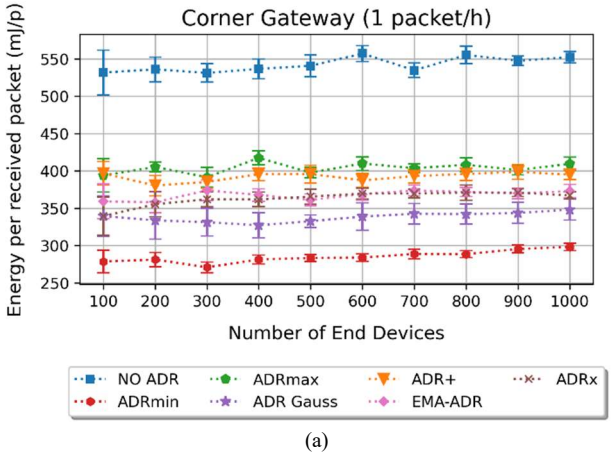

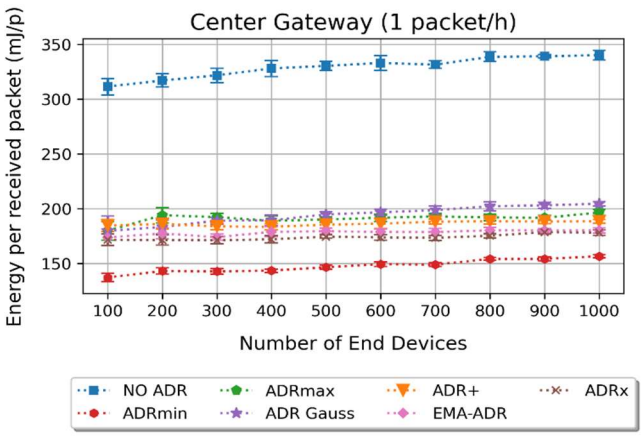

Fig. 7. Average Energy Consumption per received packet, one packet/hour. (a) corner gateway and (b) center gateway.

Moreover, ADRmax exhibits a large energy consumption per successful packet. The situation is explained by using (7) along with PDR values: if PDR decreases, then RxS decreases, increasing the energy per successfully received packet.

Fig. 8 shows the energy consumption in high traffic for both gateway locations. No ADR has the largest energy consumption in both gateway locations, similar to the low traffic case. As the number of nodes increases from 100 to 1000, energy usage per successful packet follows the same trend. The result is due the small PDR in (7), increasing energy usage.

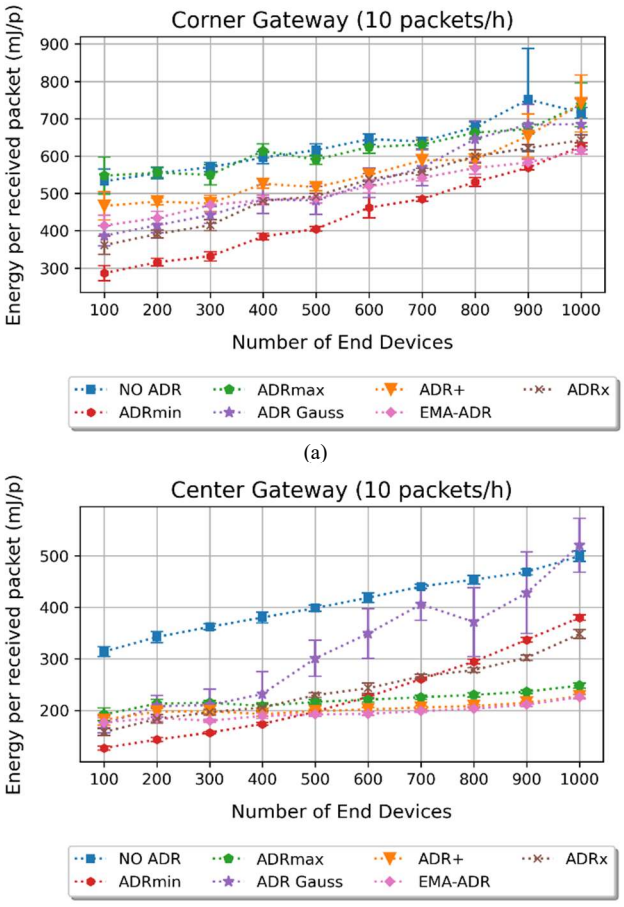

Fig. 8. Average energy consumption per received packet at a rate of 10 packets/hour. (a) corner gateway and (b) center gateway.

Regarding the other algorithms, Fig. 8 shows that ADRmin achieves small energy usage in most cases like in low traffic. Furthermore, the center gateway requires less energy than the corner because the distances are shorter in the center location.

In summary, the characteristics that improve energy usage and PDR in industrial environments relate to the link budget computation. Specifically, if the algorithm decreases the link budget with poor channel conditions, PDR increases with moderate energy usage per successful packet. On the other hand, PDR decreases when using large values of SNR for the link budget, overestimating the channel. This result is due to the variability inherent to industrial settings.

Additionally, LoRaWAN designers should favor the gateway location at the center of the area to improve PDR and energy consumption. This scenario benefits both low traffic and high traffic applications. On the other hand, if this location is not possible, the networks will decrease PDR and increase energy usage. The situation is more noticeable in high traffic applications. Furthermore, challenging propagation conditions mean PDR values smaller than 100%. ADRmin offers a good tradeoff between PDR and energy usage per successful packet regardless the type of traffic. The situation is useful when applications tolerate packet losses such as smart metering and remote equipment monitoring.

C. Total Energy usage

All values presented in the previous section show the tradeoff between energy usage and packet delivery. Therefore, some algorithms may obtain large energy usage due to a small number of received packets, consistent with (7).

Moreover, some applications may tolerate a lower PDR to decrease energy consumption. Hence, the total energy usage is an interesting metric in these cases. Table VI shows a summary of the protocols that obtain minimum and maximum total energy usage.

TABLE VI.
ADR ALGORITHMS ACCORDING TO TOTAL ENERGY USAGE.

Traffic	**Center Gateway**		**Corner Gateway**	
(PPH)	Min	Max	Min	Max
1	ADR+ ADRmax	NO ADR	ADRmax ADR+	NO ADR
10	ADRmax	NO ADR ADR Gauss	ADRmax NO ADR	ADRx

The specific values in Table VI can be computed by using (7) with Figs. 5 and 6 and their corresponding numbers in Figs. 7 and 8.

As expected, Table VI shows that No ADR exhibits the maximum energy usage in most cases. On the contrary, ADR+ and ADRmax obtain the minimum energy usage in the majority of our tests. The results seem counterintuitive compared to the previous section. Nonetheless, ADRmax and ADR+ exhibit small PDR, thus, the energy per received packet increases. Furthermore, two additional algorithms exhibit the maximum energy usage in high traffic: ADRx and ADR Gauss. Hence, both algorithms have a good PDR in high traffic at the expense of more energy consumption.

D. Recommendation for Applications

All ADR methods were tested in their original papers with variable channels and hundreds of nodes. However, the experiments included only one type of traffic and one gateway location. Thus, even if we expected improvements over ADRmax, our results show novel performance insights on all algorithms. This feature is observed especially with different traffic, providing guides to choose a specific ADR method for particular industrial applications.

Fig. 9 shows a comparison between all ADR algorithms including four dimensions: simplicity in implementation, PDR, energy savings per successfuly received packet, and scalability. The figure summarizes all results from Figs. 5 to 8 including both gateway positions and both types of traffic. This comparison helps in determining what applications will benefit from a specific ADR scheme.

According to Fig. 9, EMA-ADR, ADR+ and ADRmax show very good scalability and energy savings, but they do not offer adequate PDR values. Furthermore, ADRmin and ADRx offer the best PDR in high traffic with interesting energy savings per successful packet. However, ADRx displays small PDR in low traffic, hence, Fig. 9 shows ADRx with moderate PDR. ADRmin and ADRx exhibit poor scalability.

Additionally, considering LoRaWAN data rate and ToA, industrial applications that can benefit from the technology correspond to Non-Time Critical communications [34]. ADRmin and ADRx could benefit some high traffic applications (similar to 10 packets per hour), such as logistic processes involving inventory, or quality control, data acquisition, and remote industrial production monitoring.

Moreover, ADRmin offers a good tradeoff between PDR, energy savings and simplicity. This algorithm is an interesting alternative for low traffic applications. Examples include smart metering and periodic monitoring of variables including sound, temperature or humidity.

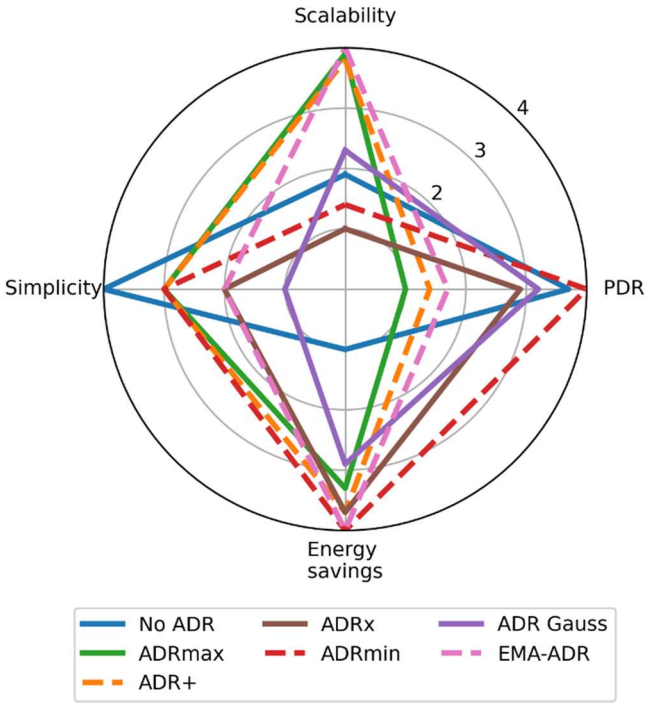

Fig. 9. ADR Algorithm comparison.

VI. Conclusions

This paper evaluates the performance of six different adaptive data rate algorithms for LoRaWAN. Tests vary the traffic and the location of the gateway to reflect diverse conditions in industrial environments. The paper computes a realistic propagation model obtained from LoRaWAN measurements in industrial settings. The model exhibits a path loss exponent and shadowing more challenging than models used in the literature. Experiments with the six ADR algorithms show a maximum of 80% PDR; thus, applications using LoRaWAN in industrial environments must tolerate packet losses. Results show that ADRmin offers a good tradeoff between PDR and energy consumption per successful packet in low traffic applications such as smart metering. When traffic increases, PDR decreases, and energy consumption increases. Nonetheless, ADRmin and ADRx provide a good tradeoff between PDR and energy usage per successful packet in high traffic scenarios. The situation may affect applications such as remote equipment monitoring. Moreover, algorithms that overestimate the channel behavior, such as ADRmax, exhibit small PDR due to the high variability of the industrial environment.

These results are helpful for network designers and researchers working in LoRaWAN implementations in industrial environments. Future work will implement these algorithms and test them using LoRaWAN nodes in actual industrial environments to confirm their usability. Future work will also test their behavior with mobile nodes.

References

[1] S. Aheleroff *et al.*, "IoT-enabled smart appliances under industry 4.0: A case study," *Advanced Engineering Informatics*, vol. 43, p. 101043, Jan. 2020, doi: 10.1016/J.AEI.2020.101043.

[2] U. Raza, P. Kulkarni, and M. Sooriyabandara, "Low Power Wide Area Networks: An Overview," *IEEE Communications Surveys and Tutorials*, vol. 19, no. 2, pp. 855–873, Apr. 2017, doi: 10.1109/COMST.2017.2652320.

[3] L. E. Marquez, M. Calle, and J. C. Velez, "Modeling LoRa: A Complex Envelope Approach," *2020 International Symposium on Networks, Computers and Communications, ISNCC 2020*, Oct. 2020, doi: 10.1109/ISNCC49221.2020.9297311.

[4] A. Augustin, J. Yi, T. Clausen, and W. M. Townsley, "A Study of LoRa: Long Range & Low Power Networks for the Internet of Things," *Sensors 2016, Vol. 16, Page 1466*, vol. 16, no. 9, p. 1466, Sep. 2016, doi: 10.3390/S16091466.

[5] M. Slabicki, G. Premsankar, and M. di Francesco, "Adaptive configuration of lora networks for dense IoT deployments," *IEEE/IFIP Network Operations and Management Symposium: Cognitive Management in a Cyber World, NOMS 2018*, pp. 1–9, Jul. 2018, doi: 10.1109/NOMS.2018.8406255.

[6] A. Farhad, D. H. Kim, S. Subedi, and J. Y. Pyun, "Enhanced LoRaWAN Adaptive Data Rate for Mobile Internet of Things Devices," *Sensors 2020, Vol. 20, Page 6466*, vol. 20, no. 22, p. 6466, Nov. 2020, doi: 10.3390/S20226466.

[7] R. Marini, W. Cerroni, and C. Buratti, "A Novel Collision-Aware Adaptive Data Rate Algorithm for LoRaWAN Networks," *IEEE Internet of Things Journal*, vol. 8, no. 4, pp. 2670–2680, Feb. 2021, doi: 10.1109/JIOT.2020.3020189.

[8] G. G. M. de Jesus, R. D. Souza, C. Montez, and A. Hoeller, "Lorawan adaptive data rate with flexible link margin," *IEEE Internet of Things Journal*, vol. 8, no. 7, pp. 6053–6061, Apr. 2021, doi: 10.1109/JIOT.2020.3033797.

[9] E. Tanghe *et al.*, "The industrial indoor channel: Large-scale and temporal fading at 900, 2400, and 5200 MHz," *IEEE Transactions on Wireless Communications*, vol. 7, no. 7, pp. 2740–2751, Jul. 2008, doi: 10.1109/TWC.2008.070143.

[10] J. Haxhibeqiri, A. Karaagac, F. van den Abeele, W. Joseph, I. Moerman, and J. Hoebeke, "LoRa indoor coverage and performance in an industrial environment: Case study," *IEEE International Conference on Emerging Technologies and Factory Automation, ETFA*, pp. 1–8, Jun. 2017, doi: 10.1109/ETFA.2017.8247601.

[11] B. Chaudhari and S. Borkar, "Design considerations and network architectures for low-power wide-area networks," *LPWAN Technologies for IoT and M2M Applications*, pp. 15–35, Jan. 2020, doi: 10.1016/B978-0-12-818880-4.00002-8.

[12] LoRa Alliance, "LoRaWAN® Specification v1.0.2 - LoRa Alliance®," 2016. https://lora-alliance.org/resource_hub/lorawan-specification-v1-0-2/ (accessed Dec. 15, 2021).

[13] M. Bor, U. Roedig, T. Voigt, and J. M. Alonso, "Do LoRa low-power wide-area networks scale?," *MSWiM 2016 - Proceedings of the 19th ACM International Conference on Modeling, Analysis and Simulation of Wireless and Mobile Systems*, pp. 59–67, Nov. 2016, doi: 10.1145/2988287.2989163.

[14] SEMTECH Corporation, "AN1200.22 LoRa™ Modulation Basics," Camarillo, CA, USA, 2015. Accessed: Jul. 14, 2022. [Online]. Available: https://www.frugalprototype.com/wp-content/uploads/2016/08/an1200.22.pdf

[15] A. Augustin, J. Yi, T. Clausen, and W. M. Townsley, "A Study of LoRa: Long Range & Low Power Networks for the Internet of Things," *Sensors 2016, Vol. 16, Page 1466*, vol. 16, no. 9, p. 1466, Sep. 2016, doi: 10.3390/S16091466.

[16] "SX1276 | 137MHz to 1020MHz Long Range Low Power Transceiver | Semtech." https://www.semtech.com/products/wireless-rf/lora-core/sx1276#datasheets (accessed Jun. 03, 2022).

[17] Semtech Corporation, "Lora networks Rate adaptation Class A/B specification: LoRaWAN-simple rate adaptation recommended algorithm," Oct. 2016. [Online]. Available: www.semtech.comwww.semtech.com

[18] J. Babaki, M. Rasti, and S. K. Taskou, "Improved Configuration of transmission variables for LoRaWAN in High-Noise Channels," *2020 28th Iranian Conference on Electrical Engineering, ICEE 2020*, Aug. 2020, doi: 10.1109/ICEE50131.2020.9260713.

[19] Y. Li, J. Yang, and J. Wang, "DyLoRa: Towards Energy Efficient Dynamic LoRa Transmission Control," *Proceedings - IEEE INFOCOM*, vol. 2020-July, pp. 2312–2320, Jul. 2020, doi: 10.1109/INFOCOM41043.2020.9155407.

[20] A. Peruzzo and L. Vangelista, "A Power Efficient Adaptive Data Rate Algorithm for LoRaWAN networks," *International Symposium on Wireless Personal Multimedia Communications, WPMC*, vol. 2018-November, pp. 90–94, Jul. 2018, doi: 10.1109/WPMC.2018.8713092.

[21] J. Finnegan, R. Farrell, and S. Brown, "Analysis and Enhancement of the LoRaWAN Adaptive Data Rate Scheme," *IEEE Internet of Things Journal*, vol. 7, no. 8, pp. 7171–7180, Aug. 2020, doi: 10.1109/JIOT.2020.2982745.

[22] J. Babaki, M. Rasti, and R. Aslani, "Dynamic spreading factor and power allocation of lora networks for dense IoT deployments," *IEEE International Symposium on Personal, Indoor and Mobile Radio Communications, PIMRC*, vol. 2020-August, Aug. 2020, doi: 10.1109/PIMRC48278.2020.9217283.

[23] S. Li, U. Raza, and A. Khan, "How Agile is the Adaptive Data Rate Mechanism of LoRaWAN?," *2018 IEEE Global Communications Conference, GLOBECOM 2018 - Proceedings*, 2018, doi: 10.1109/GLOCOM.2018.8647469.

[24] V. Hauser and T. Hegr, "Proposal of adaptive data rate algorithm for LoRaWAN-based infrastructure," *Proceedings - 2017 IEEE 5th International Conference on Future Internet of Things and Cloud, FiCloud 2017*, vol. 2017-January, pp. 85–90, Nov. 2017, doi: 10.1109/FICLOUD.2017.47.

[25] P. Tempiem and R. Silapunt, "Quantile Classification of Variance from the Mean for Spreading Factor Allocation in LoRaWAN," *InCIT 2020 - 5th International Conference on Information Technology*, pp. 179–184, Oct. 2020, doi: 10.1109/INCIT50588.2020.9310964.

[26] D. Todoli, J. Silvestre, V. Sempere, and A. Planes, "Analysis of Bidirectional ADR-Enabled Class B LoRaWAN Networks in Industrial Scenarios," *Applied Sciences 2020, Vol. 10, Page 7964*, vol. 10, no. 22, p. 7964, Nov. 2020, doi: 10.3390/APP10227964.

[27] E. Sisinni, A. Saifullah, S. Han, U. Jennehag, and M. Gidlund, "Industrial Internet of Things: Challenges, Opportunities, and Directions," *IEEE*

Transactions on Industrial Informatics, vol. 14, no. 11, pp. 4724–4734, Nov. 2018, doi: 10.1109/TII.2018.2852491.

[28] A. Osorio, M. Calle, J. D. Soto, and J. E. Candelo-Becerra, "Routing in LoRaWAN: Overview and Challenges," *IEEE Communications Magazine*, vol. 58, no. 6, pp. 72–76, Jun. 2020, doi: 10.1109/MCOM.001.2000053.

[29] D. A. Wassie, I. Rodriguez, G. Berardinelli, F. M. L. Tavares, T. B. Sørensen, and P. Mogensen, "Radio Propagation Analysis of Industrial Scenarios within the Context of Ultra-Reliable Communication," *IEEE Vehicular Technology Conference*, vol. 2018-June, pp. 1–6, Jul. 2018, doi: 10.1109/VTCSPRING.2018.8417469.

[30] L. Leonardi, F. Battaglia, G. Patti, and L. lo Bello, "Industrial Lora: A novel medium access strategy for Lora in industry 4.0 applications," *Proceedings: IECON 2018 - 44th Annual Conference of the IEEE Industrial Electronics Society*, pp. 4141–4146, Dec. 2018, doi: 10.1109/IECON.2018.8591568.

[31] E. Sisinni *et al.*, "LoRaWAN Range Extender for Industrial IoT," *IEEE Transactions on Industrial Informatics*, vol. 16, no. 8, pp. 5607–5616, Aug. 2020, doi: 10.1109/TII.2019.2958620.

[32] M. Jimenez *et al.*, "Obstacles, Speed and Spreading Factor: Insights in LoRa Mobile Performance," *International Journal on Communications Antenna and Propagation (IRECAP)*, vol. 9, no. 3, pp. 228–235, Jun. 2019, doi: 10.15866/IRECAP.V9I3.17296.

[33] LoRa Alliance Technical Committee Regional Parameters Workgroup, "LoRaWAN 1.1 Regional Parameters 2, Revision B," 2018. Accessed: Jan. 13, 2019. [Online]. Available: https://lora-alliance.org/sites/default/files/2018-04/lorawantm_regional_parameters_v1.1rb_-_final.pdf

[34] P. Varga *et al.*, "5G support for Industrial IoT Applications— Challenges, Solutions, and Research gaps," *Sensors*, vol. 20, no. 3, p. 828, Feb. 2020, doi: 10.3390/s20030828.

Angelo Soto-Vergel graduated with a BS degree in Electronics Engineering at the Francisco de Paula Santander University, Cucuta, Colombia, in 2013. Then he graduated with a specialist degree in Advanced Technologies for the Development of Software at the Autonomous University of Bucaramanga, Bucaramanga, Colombia, in 2016. Then he graduated with a technologist degree in Analysis and Development of Information Systems at the Servicio Nacional de Aprendizaje, Bogota, Colombia, in 2017. He graduated with a Master's degree in Mathematics Education from the Francisco de Paula Santander University in Cucuta, Colombia, in 2019. Currently, he is pursuing doctoral studies in Electrical and Electronic Engineering at the Fundacion Universidad del Norte, Barranquilla, Colombia. His research interests include the analysis, application, and development of communications systems that integrate LPWAN and TinyML technologies.

Luis Arismendy received a BS degree in electronics engineering from Universidad del Norte, Barranquilla, Colombia, in 2020. He also graduated from the MS program in electronics engineering at the same university in 2022. He is an Adjunct Professor at the Electrical and Electronics Engineering Department, Universidad del Norte, Barranquilla, Colombia. His research interests include data analytics, artificial intelligence, and communication technologies for wireless sensor networks.

Robinson Bornacelli-Durán received the BS degree in electronics engineering from Universidad del Norte, Barranquilla, Colombia, in 2004. He obtained a MS degree in electronics engineering at the same university. He is a support engineer in an important company in Colombia. His research interests include robotics, artificial intelligence, and radio communication and signals.

Carlos Cardenas received the BS degree in Mechanical Engineering and Electronics Engineering from Universidad del Norte, Barranquilla, Colombia, in 2020. He obtained a MS degree in electronics engineering at the same university. He is a teaching assistant with the Electrical and Electronics Engineering Department, Universidad del Norte, Barranquilla, Colombia. His research interests include signal processing, data analysis, artificial intelligence and robotics.

Brayan Montero-Arévalo graduated with a BS degree in mechatronics engineering at Santo Tomas University, Bucaramanga, Colombia in 2017 and Ed.S. in Industrial automation in 2019 at the same university. Since 2020, he is pursuing his MS in electronics engineering at Universidad del Norte, Barranquilla, Colombia. He is a professor at Universidad Nacional de Colombia with the engineering department. His actual research is focused on biosensors and biomarkers.

Emanuel Rivera received the BS degree in electronics engineering from Universidad del Norte, Barranquilla, Colombia, in 2021. He is currently pursuing the MS degree in electronics engineering at the same university. He is a teaching assistant with the Electrical and Electronics Engineering Department, Universidad del Norte, Barranquilla, Colombia. His research interests include robotics and Web development.

Maria Calle (SM '14) received the BS degree in electronics engineering from Universidad Pontificia Bolivariana, Medellín, Colombia, 1995, and the MS degree in telecommunications and the Ph.D. degree in information sciences from the University of Pittsburgh, Pittsburgh, PA, USA, in 2006 and 2009, respectively. She is a Professor with the Universidad del Norte, Barranquilla, Colombia. She is a Senior Researcher in Minciencias, Bogota, Colombia, and the Coordinator of the Telecommunications and Signals Research Group, Universidad del Norte in Barranquilla. Her current research interests include low power wide area networks, communication protocols for Internet of Things, and engineering education.

John E. Candelo-Becerra received his Bachelor degree in Electrical Engineering in 2002 and his Ph.D. in Engineering with an emphasis in Electrical Engineering in 2009 from Universidad del Valle, Cali, Colombia. His employment experience includes the Empresa de Energía del Pacífico EPSA, Universidad del Norte, and Universidad Nacional de Colombia - Sede Medellín. He is now an Associate Professor at the Universidad Nacional de Colombia, Sede Medellín, Colombia. He is a Senior Researcher in Minciencias-Colombia and a member of the Applied Technologies Research Group – GITA at the Universidad Nacional de Colombia. His research interests include engineering education; planning, operation, and control of power systems; artificial intelligence; smart grids; and microgrids.